Particle
& Particle Systems Characterization
www.particle-journal.com

Concurrent Detection of Protein Adsorption on Mixed Nanoparticles by Differential Centrifugal Sedimentation

*Ruimin Wang, Lan Chen, Dexing Li, Renxiao Liu, and Guanglu Ge**

In mixtures of nanoparticles of various sizes or compositions, monitoring protein partitioning on their surfaces provides important information about particle–protein interactions during competitive adsorption. Utilizing the size-resolving capability of differential centrifugal sedimentation, the adsorption of bovine serum albumin on multisize gold nanoparticles with diameters ranging from 20 to 100 nm or gold, silver, and silica nanoparticles with similar diameter can be concurrently observed. This method can be used to gain insight into nanoparticle–protein interactions based on analyses of curvature and relative abundance.

Understanding the interface between nanoparticles (NPs) and biomolecules is of profound importance for bio-nanotechnology applications.[1] Accordingly, extensive research has focused on quantifying protein adsorption on NP surfaces, i.e., the protein corona (PC), in a biological medium.[2] Based on analyses using dynamic light scattering (DLS), atomic force microscopy, and other methods,[3] PC formation is mainly determined by properties of the NP and protein, with media composition and incubation conditions also playing roles.[4] Substantial progress has been made in determining correlations between PC structures and nanoparticle properties, e.g., size, shape, surface charge, and surface curvature[4b,c,5] owing to the availability of the well-defined NPs and precise control over their morphologies and surface functionalization.

Most studies on the PC use monodisperse NPs for simplicity. In reality, biological media are likely to contact polydisperse NPs, either with varying compositions or aggregation states. Hence, the development of new methods to simultaneously analyze several aspects of NP–protein interactions is necessary.[1b] Comparisons of the competitive capability of various NPs to attract proteins in the same solution may facilitate practical applications of NPs in biological fluids, but cannot be achieved using model NPs.[6]

Differential centrifugal sedimentation (DCS) is based on the correlation between particle size and sedimentation velocity in fluids with a density gradient,[7] and has become a precise and powerful method for particle sizing.[8] Owing to its superb size-resolving capability with particle size resolution of 3%, it has been utilized to identify particles with slightly different size in a mixture. For example, dimers, trimers, and aggregates of higher order could be resolved with high precision.[9] The method also enables the characterization of NP–protein composites in a quantitative manner in the presence of a complex protein mixture.[1a] Accordingly, the method has been used to measure subtle size difference before and after the adsorption of ligands on NPs.[10] Bell et al. noted that DCS can provide precise measurements of the thickness of complete protein shells on dense NPs, similar to analytical ultracentrifugation.[3b]

In this work, we demonstrate the feasibility of examining biomolecule–NP interactions in a mixed nanoparticle system by DCS, both for the difference among NPs and that for protein adsorption. The influence of NP surface curvature on the thickness of the shell formed by bovine serum albumin (BSA), a model serum carrier protein with 76% sequence identity with human serum albumin,[11] was investigated. We also expand the method to measure the mixed NPs with different composition (density).

Aqueous solutions of citrate-stabilized gold nanoparticles (GNPs) with six nominal sizes, i.e., 20, 30, 40, 60, 80, and 100 nm, were prepared. The concentration of these solutions was adjusted so that NPs of different sizes had similar total surface areas without aggregation. The mixture of GNPs with different diameters was added to a BSA solution at various concentrations (from 10^{-15} to 10^{-3} mol L^{-1}) and incubated at 37 °C for 60 min, which is sufficient for BSA adsorption on citrate-stabilized GNPs.[11] No significant aggregation was observed in our samples, simplifying data interpretation.

The mixed GNPs with different diameters were analyzed by DCS before and after incubation with BSA respectively. First of all, the GNP mixture with six diameters of 18.00, 29.00, 39.00, 58.67, 86.33, and 111.00 nm, has been measured, as shown in Figure S1 in the Supporting Information. The principle of this method has been explained in Supporting Information. This experimentally determined diameter value is used for the subsequent calculations in this work. In CPS centrifugation experiments, the BSA shell, formed by BSA molecules binding on the GNPs, moved with GNPs during sedimentation. **Figure 1** presents the Stokes diameters of the GNPs as a function of BSA concentration. Peaks corresponding to the six diameters could be clearly resolved, and observed to shift, without observable peaks from agglomerated NPs. This feature

R. Wang, Dr. L. Chen, Dr. D. Li, Dr. R. Liu, Prof. G. Ge
CAS Key Laboratory of Standardization and Measurement for Nanotechnology and CAS Center for Excellence in Nanoscience
National Center for Nanoscience and Technology
Beijing 100190, China
E-mail: gegl@nanoctr.cn

DOI: 10.1002/ppsc.201700134

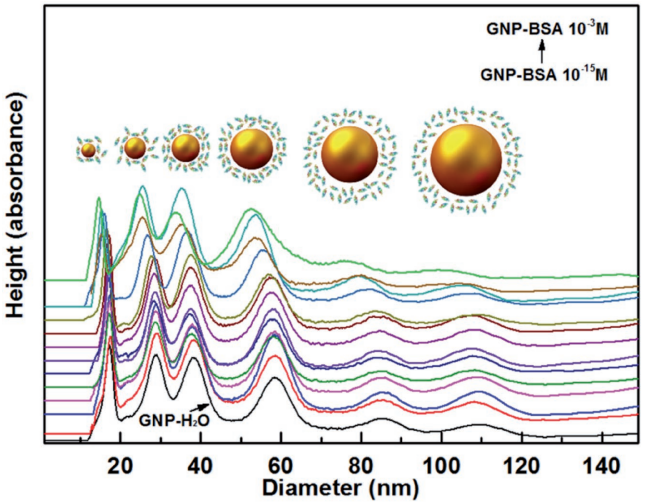

Figure 1. The Stokes diameters of mixed GNPs and mixed GNP-BSA for a series of concentrations.

is suitable for monitoring protein adsorption in a mixture of GNPs simultaneously in a single experiment. Although DLS is commonly used to characterize NPs and to analyze protein and NP absorption,[3a] it does not have sufficient resolution for monitoring differently sized particles in a mixture (Figure S2, Supporting Information). Taking the peaks obtained for GNP–H_2O (without BSA) as a benchmark, peaks for all measured apparent diameters (d_m) shifted systematically toward slightly smaller values with increasing BSA concentrations. This is because that the average density of GNP–BSA shell was smaller than that of the GNPs, and the settling time recorded by DCS was longer, which suggested the settling velocity was slower than that of GNPs. Therefore, the apparent diameters of GNP–BSA were smaller than GNPs due to the software calculation according to the Equation S2 in the Supporting Information, by using the density of GNPs. Moreover, the larger the BSA concentration, the smaller the apparent diameters measured by DCS. This agrees with the expectation that BSA, binding to GNPs increases as the concentration increase, the average density of GNP–BSA becomes smaller and smaller.

The settling time of GNP–BSA shell was credible which has been directly recorded by the detector. The settling time as a function of the BSA concentration is shown in Figure S3 in the Supporting Information. In general, the settling time increased with increasing BSA concentration, indicating that the protein coating on GNPs was thicker. This is consistent with previous studies showing that protein-coated NPs have a lower average density and larger diameter, and result in a net increase in the sedimentation time.[12] When the BSA concentration is low, the settling time increases gradually, suggesting partial protein coverage on the GNP and relatively few BSA molecules coating on the GNP. Therefore, the settling time is close to that of the GNP. Similar results have been described for IgG protein adsorption on GNPs.[3b] In high concentration, the retarding effect caused by the protein adsorption is significant and the settling time increases substantially. Moreover, the BSA shell had a greater influence on small GNP (especially 20 nm) sedimentation than that of larger NPs; since the hydrodynamic size of BSA is comparable to the size of NPs, the average density is reduced dramatically.

To verify the existence of the BSA shell on GNP surfaces, the samples were characterized by transmission electron microscope (TEM). As shown in Figure S4 in the Supporting Information, GNPs with different sizes were observed. The BSA shell is detected on the external surfaces of GNPs. Moreover, it is clear to see the BSA shell capped on the GNPs. However, TEM is not able to scrutinize the GNP–BSA samples at high BSA concentration; as this method cannot provide reliable information to study the protein shell owing to the low contrast among organic materials.[13]

A theoretical framework has been established to extract thickness of BSA shell information from DCS data. Following previous reports and assuming a spherical core/shell model for the protein-coated particles,[3b,12b] we define the BSA shell with a thickness l as the shell and GNPs with a diameter d_c as the core, as shown in Scheme S2 in the Supporting Information. The thickness of the BSA shell is calculated based on density values obtained from the literature.[14] In this work, the sedimentation of spherical core/shell model was analyzed in the Supporting Information. Finally, the function including the l has been obtained, as shown in Equation S7 in the Supporting Information. Therefore the l was calculated by using this Equation S7 in the Supporting Information. The data of shell thickness have been shown in **Figure 2**. The thickness of the BSA shell on GNPs was small and increased slowly for low protein concentrations, i.e., below 10^{-8} M. The thickness increased rapidly for higher protein concentrations. As discussed above, protein coverage on GNPs is believed to be partial at low protein concentrations; accordingly, centrifugal fluid flow redistributes BSA to the unoccupied area of the GNP to reduce

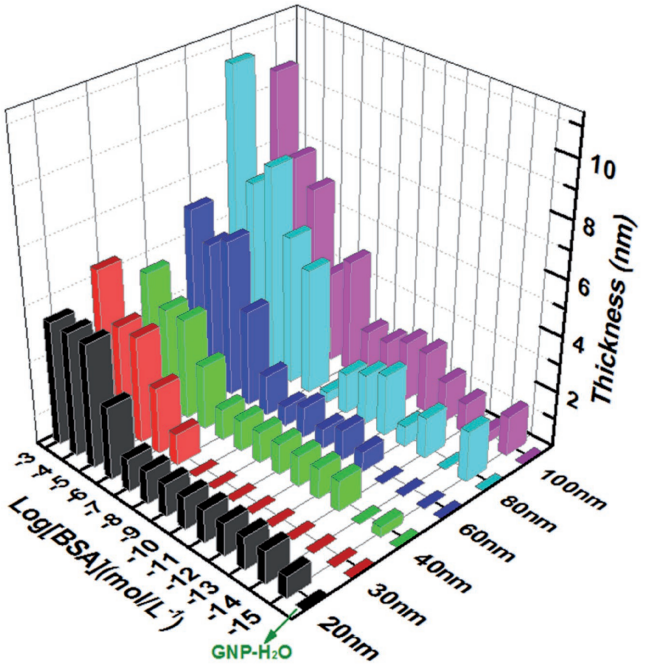

Figure 2. The BSA shell thickness for mixed GNPs of every diameter after incubation with various concentrations of BSA.

the drag force.[3b] BSA experiences partial deformation during the sedimentation process. This explains the fluctuation in corona thickness around 1–2 nm. These results are consistent with those of Jachimska et al.,[14] who showed that the maximum height of individual BSA adsorbed on a silica chip was 1.0 ± 0.2 nm. This suggests that BSA only formed a monomolecular layer on the GNP surface at low concentrations.

For high protein concentrations, as GNPs were coated with more BSA molecules, the BSA shell can get stiff and is not easily deformable by the fluid flow. A significant increase of BSA shell thickness is observed when the number of protein molecules relative to the number of GNPs is high. Importantly, a difference in protein thickness among GNPs of different sizes is observed. For small GNPs, the BSA is immediately adsorbed on the NP surfaces and formed a monomolecular BSA shell around the GNP surface at the low concentrations; smaller GNPs with high curvature induce the formation of a loose protein layer and rapidly established sorption equilibrium.[3b] Therefore, the BSA shell is almost invariable until the protein concentration reaches 10^{-7}M. The BSA shell of all GNPs is thickened rapidly as the protein concentration increases and multilayer adsorption is dominant, which suggests that the GNPs with larger diameter are found more favorable to bind BSA in mixed GNPs system.

These results reveal that the BSA shell is thicker on large GNPs than that on small GNPs on the whole. This point is supported by previous results. Forrest and co-workers have studied the denaturing kinetics of BSA adsorbed on GNPs and found that the BSA surface coverage is much lower on small spheres than on large spheres, and attributed this to the loss of the BSA tertiary structure.[15] A similar phenomenon has been described by Ge and co-workers[16] and Kundu and co-workers.[17] Moreover, at the maximum concentration, the shell thickness on GNPs of 30 nm was larger than that of 40 nm GNPs, while that of GNPs of 80 nm was larger than that of 100 nm GNPs. These differences may be attributed to the difference in the degree of compliance with the curvature of the particle surface and the structure of BSA. In addition, we measured the zeta potential of the six sized NP. The values are −32.6, −40.5, −37.2, −40.6, −47.5, −42 mV for GNPs with size from 20 to 100 nm, respectively. From the perspective of zeta potential, the GNPs with more negative charge tend to bind more BSA molecules, owing to the positively charged amino acid residues of BSA.[18]

The high size resolution of DCS which has achieved the size resolution of 0.2 nm in analyzing Au clusters[19] is able to realize to distinguish GNPs of different diameter in the mixture and the tiny difference among the thicknesses of protein shell binding to GNPs. However, this method has a unique feature that all samples have to be subjected to centrifugal force. Centrifugation may affect the BSA shell, since the protein molecules may become denser in order to reduce the drag force in the process of centrifugal movement. It is important to note that the thickness of the BSA shell is calculated based on settlement, not in the stationary and free state. Therefore, the calculated thicknesses may be smaller than values determined by other technologies. For example, the protein thickness was 8–10 nm for GNP size from 12 to 80 nm and increased to 15–16 nm for GNP size from 100 to 150 nm in which the value of hydrodynamic diameter was measured by DLS.[20]

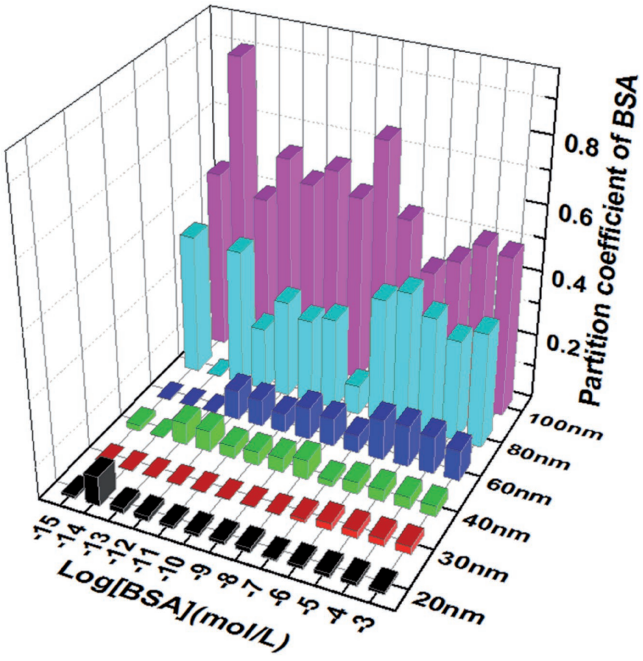

Figure 3. Partition coefficients of BSA molecules adsorbed on GNPs after incubation with BSA at a series of concentrations.

By assuming the fully covered BSA shell, hence, the mass of BSA shell could be obtained by a straightforward calculation in case of knowing the thickness of BSA shell capped on GNP. Therefore, the number of BSA molecules adsorbed on GNPs can be calculated according to that the mass of BSA shell divided by the molar mass of BSA molecule and multiplied by Avogadro's constant. By comparing the number of BSA molecules per unit surface area on GNPs (Figure S5, Supporting Information), the GNP adsorbed more protein molecules for high protein concentrations, and larger GNPs always adsorbed more molecules, that was consistent with the above discussion. We have observed that the partition coefficients of BSA molecules adsorbed on GNPs of sizes 20, 30, and 40 nm were smaller than that on GNPs of 80and 100 nm as shown in **Figure 3**. People were interested in the size-dependent protein adsorption on NPs for a long time. Piella et al.[20] have reported that the first proteins binding on NPs served as nucleation center to deposit and stabilize more proteins. Most assumptions and explanations about the formation of PC referred that the initial adsorbed proteins have experienced rearrangements to make the adsorption stable and then form irreversible adsorption. However, the small NPs with limited surface restricted this process of protein rearrangement. Moreover, the higher surface curvature of smaller GNPs leads to proteins separate from each other, and makes the adsorption of further BSA more difficult.[21] Based on our experiment result and the discussion from literature, we speculated that the smaller NP was more capable in resisting nonspecific adsorption.

The ability to monitor protein partitioning simultaneously on GNP surfaces provides direct information about competitive adsorption. The protein partition coefficient was calculated according to that the number of BSA molecule on GNP with one size divided by the sum of number of BSA on GNP with

six size. Hence, the partition coefficient of BSA molecules adsorbed on GNPs of different size is described in Figure 3. The partition coefficient of BSA is small and unchanging for small GNPs. However, the partition coefficient is larger and subject to change for large GNPs. This reveals that protein molecules tend to be adsorbed on large NPs. The trend on the interaction of NPs with proteins are still worth examining, but the estimates will be greater than the actual values owing to the assumptions of the analysis.

In addition, we speculated that this method can distinguish different kinds of NP mixtures based on its high sensitivity. Therefore, we used a mixture of three kinds of NPs with similar size but different density to measure the settling time before and after incubation with BSA, as shown in Figures S6–S9 in the Supporting Information. The settling time of the mixture with the BSA shell is slower than that of each category of NPs in the mixture. Additionally, the smaller the nanoparticle density, the slower the settling velocity, i.e., NPs with smaller density are more affected by coated protein shells in the sedimentation. Combined with the results presented in Figure S3 in the Supporting Information, sedimentation of NPs with relatively small size or density is more severely affected by the formation of the BSA shell.

We demonstrated the potential application of DCS in simultaneously detection of protein adsorbed NPs in a mixture. Under identical conditions, protein molecules tend to be adsorbed on large NPs. Resistance to nonspecific adsorption may explain, at least in part, why small NPs are more suitable for biomedical applications. Furthermore, the fluid dynamics of NPs with smaller size or density is more severely affected by the BSA shell. These findings provide insight into the interactions of proteins and multisize NPs of different size and density. This opens a door for direct observations of BSA shell formation under competitive environment, and can be applied to a wide range of NPs and protein systems.

Experimental Section

Reagents and Chemicals: Citrate-stabilized GNPs with nominal diameters of 20, 30, 40, 60, 80, and 100 nm were purchased from BBI International Ltd. (Cardiff, UK). Sucrose was purchased from Alfa Aesar Co., Ltd. (Tianjin, China). BSA was purchased from Sigma-Aldrich (St. Louis, MO, USA). Standard NPs of silicon dioxide (SiO_2, 150 nm) for calibration were provided by the China University of Petroleum.

Apparatus: All nanoparticle images were obtained using an FEI Tecnai G2 20 S-TWIN transmission electron microscope operated at an accelerating voltage of 200 kV. The measurement of hydrodynamic diameter and zeta potential of GNPs were performed using a Zetasizer Nano ZS (Malvern Instruments).

DCS was performed using a DC24000 UHR Disc Centrifuge nanoparticle size analyzer (CPS Instruments, Inc., Prairieville, LA, USA). The instrument was operated at 24 000 rpm with 14.4 mL of sucrose solution in a gradient of 8–24% (average gradient density between the point of injection and detection was 1.06 g cm^{-3}). In all cases, DI water was prepared using the D-Q5 Pure/Ultrapure System (Merck Millipore, Darmstadt, Germany).

Supporting Information

Supporting Information is available from the Wiley Online Library or from the author.

Acknowledgements

This work was supported by the Strategic Priority Research Program of the Chinese Academy of Sciences, Grant No. XDA09040400. The National Key Research and Development Program of China, Grant No. 2016YFA0200904.

Conflict of Interest

The authors declare no conflict of interest.

Keywords

bovine serum albumin shell, competitive adsorption, differential centrifugal sedimentation, gold nanoparticles

Received: April 10, 2017
Revised: September 6, 2017
Published online:

[1] a) M. Mahmoudi, I. Lynch, M. R. Ejtehadi, M. P. Monopoli, F. B. Bombelli, S. Laurent, *Chem. Rev.* **2011**, *111*, 5610; b) V. Forest, J. Pourchez, *Nano Today* **2016**, *11*, 700; c) D. Docter, D. Westmeier, M. Markiewicz, S. Stolte, S. K. Knauer, R. H. Stauber, *Chem. Soc. Rev.* **2015**, *44*, 6094; d) F. Zhao, Y. Zhao, Y. Liu, X. Chang, C. Chen, Y. Zhao, *Small* **2011**, *7*, 1322.

[2] T. Cedervall, I. Lynch, S. Lindman, T. Berggard, E. Thulin, H. Nilsson, K. A. Dawson, S. Linse, *Proc. Natl. Acad. Sci. USA* **2007**, *104*, 2050.

[3] a) M. H. Cui, R. X. Liu, Z. Y. Deng, G. L. Ge, Y. Liu, L. M. Xie, *Nano Res.* **2014**, *7*, 345; b) N. C. Bell, C. Minelli, A. G. Shard, *Anal. Methods* **2013**, *5*, 4591; c) S. Y. Zhang, Y. Moustafa, Q. Huo, *ACS Appl. Mater. Interfaces* **2014**, *6*, 21184; d) A. Patra, T. Ding, G. Engudar, Y. Wang, M. M. Dykas, B. Liedberg, J. C. Kah, T. Venkatesan, C. L. Drum, *Small* **2016**, *12*, 1174.

[4] a) M. Lundqvist, J. Stigler, G. Elia, I. Lynch, T. Cedervall, K. A. Dawson, *Proc. Natl. Acad. Sci. USA* **2008**, *105*, 14265; b) E. Casals, T. Pfaller, A. Duschl, G. J. Oostingh, V. Puntes, *ACS Nano* **2010**, *4*, 3623; c) W. G. Kreyling, S. Fertsch-Gapp, M. Schaffler, B. D. Johnston, N. Haberl, C. Pfeiffer, J. Diendorf, C. Schleh, S. Hirn, M. Semmler-Behnke, M. Epple, W. J. Parak, *Beilstein J. Nanotechnol.* **2014**, *5*, 1699.

[5] a) S. Khan, A. Gupta, A. Chaudhary, C. K. Nandi, *J. Chem. Phys.* **2014**, *141*, 084707; b) W. Shang, J. H. Nuffer, V. A. Muniz-Papandrea, W. Colon, R. W. Siegel, J. S. Dordick, *Small* **2009**, *5*, 470.

[6] I. Lynch, K. A. Dawson, *Nano Today* **2008**, *3*, 40.

[7] R. M. Wang, Y. L. Ji, X. C. Wu, R. X. Liu, L. Chen, G. L. Ge, *RSC Adv.*, **2016**, *6*, 43496.

[8] Z. Krpetic, I. Singh, W. Su, L. Guerrini, K. Faulds, G. A. Burley, D. Graham, *J. Am. Chem. Soc.* **2012**, *134*, 8356.

[9] N. A. Belsey, A. G. Shard, C. Minelli, *Biointerphases* **2015**, *10*, 019012.

[10] a) D. Di Silvio, N. Rigby, B. Bajka, A. Mayes, A. Mackie, F. B. Bombelli, *Nanoscale* **2015**, *7*, 11980; b) P. M. Kelly, C. Aberg, E. Polo, A. O'Connell, J. Cookman, J. Fallon, Z. Krpetic, K. A. Dawson, *Nat. Nanotechnol.* **2015**, *10*, 472.

[11] D. C. Carter, J. X. Ho, *Adv. Protein Chem.* **1994**, *45*, 153.

[12] a) M. P. Monopoli, D. Walczyk, A. Campbell, G. Elia, I. Lynch, F. B. Bombelli, K. A. Dawson, *J. Am. Chem. Soc.* **2011**, *133*, 2525; b) A. Sikora, A. G. Shard, C. Minelli, *Langmuir* **2016**, *32*, 2216.

[13] R. P. Carney, J. Y. Kim, H. F. Qian, R. C. Jin, H. Mehenni, F. Stellacci, O. M. Bakr, *Nat. Commun.* **2011**, *2*, 1.

[14] B. Jachimska, K. Tokarczyk, M. Łapczyńska, A. Puciul-Malinowska, S. Zapotoczny, *Colloids Surf., A* **2016**, *489*, 163.
[15] J. H. Teichroeb, J. A. Forrest, L. W. Jones, *Eur. Phys. J. E*, **2008**, *26*, 411.
[16] X. J. Cheng, X. Tian, A. Q. Wu, J. X. Li, J. Tian, Y. Chong, Z. F. Chai, Y. L. Zhao, C. Y. Chen, C. C. Ge, *ACS Appl. Mater. Interfaces* **2015**, *7*, 20568.
[17] K. Das, S. Kundu, *Colloids Surf., A* **2015**, *468*, 56.
[18] A. S. Sharma, M. Ilanchelian, *J. Phys. Chem. B* **2015**, *119*, 9461.
[19] Z. Krpetic, A. M. Davidson, M. Volk, R. Levy, M. Brust, D. L. Cooper, *ACS Nano* **2013**, *7*, 8881.
[20] J. Piella, N. G. Bastús, V. Puntes, *Bioconjugate Chem.* **2017**, *28*, 88.
[21] a) X. N. Zhang, J. T. Zhang, F. Zhang, S. N. Yu, *Nanoscale* **2017**, *9*, 4787; b) S. Lindman, I. Lynch, E. Thulin, H. Nilsson, K. Dawson, S. Linse, *Nano Lett.* **2007**, *7*, 914.

